

The influence of deformation bands upon fluid flow using profile permeametry and positron emission tomography

S.R. Ogilvie, J.M. Orribo,¹ and P.W.J. Glover

Department of Geology and Petroleum Geology, University of Aberdeen, Aberdeen, Scotland

Abstract. Cataclastic deformation bands are significant discontinuities in sandstone reservoirs since they have dramatically reduced porosity and permeability relative to their host rock, despite their mm-scale displacements. Consequently, these discontinuities often have a large impact upon the flow of fluids at both micro and macro-scales. The effect of this impact in highly porous sandstone has been analyzed using a range of novel and conventional techniques, including pressure decay profile permeametry (PDPK) and positron emission tomography (PET). There are greater reductions in PDPK permeability in deformation bands relative to their host rock compared to conventional nitrogen permeametry measurements. This apparent discrepancy is the outcome of the higher spatial resolution of PDPK technique in measurements of much smaller rock volumes. There are greater porosity reductions using image analysis than conventional core techniques. These changes are reflected in a significant increase in irreducible water saturations (S_{wi}) in deformation bands indicating much reduced fluid storage capacities. PET was used to monitor fluid flow as a function of pore volume of a sandstone plug containing deformation bands, demonstrating the direct effect of deformation bands as a potential barrier to fluid flow. The results of this study provide a detailed characterization of deformation bands at high resolution, which can be included in advanced reservoir simulation models.

1. Introduction

Deformation bands are thin laterally continuous structures characterized by localized cataclasis and/or compaction [Aydin, 1978; Pittman, 1981; Antonellini and Aydin, 1994], and are commonly found in abundance in close proximity to major faults [Beach *et al.*, 1999]. Deformation bands can partially or completely compartmentalize hydrocarbon and water reservoirs, contributing to significant reservoir heterogeneity, as a result of their considerable length [Fossen and Hesthammer, 1998] and their low porosities and permeabilities [Antonellini and Aydin, 1994].

The effects of deformation bands upon petrophysical parameters have been studied using relatively low resolution techniques such as conventional core analysis [Antonellini and Aydin, 1994], scanning electron microscopy (SEM) and cathodoluminescence (CL) [Fisher and Knipe, 1998]. However, we have analyzed a range of petrophysical

parameters across cataclastic deformation bands in the Late Permian Hopeman Sandstone (Inner Moray Firth Basin, Scotland) using several novel techniques, supported by conventional measurements.

Image analysis of optical thin sections and pressure decay profile permeametry (PDPK) were used to map porosity and permeability respectively across 2D cross-sections of samples containing deformation bands. Positron emission tomography (PET) scanning was used to analyze the fluid distribution and track the fluid flow through a core plug containing deformation bands. This technique is however normally used for medical purposes such as monitoring blood flow through the body [Ashcroft *et al.*, 1992; Besson *et al.*, 1992]. Conventional helium porosimetry, mercury injection capillary pressure measurements (MICP), and nitrogen gas permeametry were used to provide supporting data in the form of porosity, klinkenberg permeability (K_L), capillary pressure and irreducible water saturation determinations (S_{wi}). Observations of porosity and permeability variation across deformation bands were made using a scanning electron microscope in backscattered electron imaging mode (SEM-BSEI).

2. Geological Setting

The Late Permian Hopeman Sandstone is located on the southern shores of the Inner Moray Firth Basin, Scotland. It is a well-sorted, porous, quartz cemented sandstone of aeolian origin. In the study area at Cummingstown foreshore [NJ132639] it is host to a damage zone of cataclastic deformation bands around the regional-scale Lossiemouth Fault. These extensional structures have much reduced permeability and porosity relative to the host sandstone and they dramatically increase in frequency towards the Lossiemouth Fault [S.R. Ogilvie *et al.*, manuscript in preparation, 2000]. The faulting occurred predominately in the Jurassic [Frostick *et al.*, 1988] and the fault systems have subsequently been reactivated allowing the passage of fluids and precipitation of cements, according to the two-stage reactivation model of Edwards *et al.* [1993].

3. Procedure and methodology

Pressure decay profile permeametry (PDPK) measurements involve placing a probe against the sample which injects into the rock a known volume of nitrogen gas at a defined gas pressure. The decay of gas pressure is monitored as the gas flows away through the rock, and this pressure decay is used to calculate a slip-corrected (klinkenberg) permeability for the rock at the given position. Blocks of highly porous sandstone containing zones of deformation bands were sawn to provide flat surfaces, which were then photographed (e.g., Fig. 1a). Centimeter grids were pencilled onto the samples so that

¹Now at Petroleum of Venezuela (PDVSA), Caracas, Venezuela

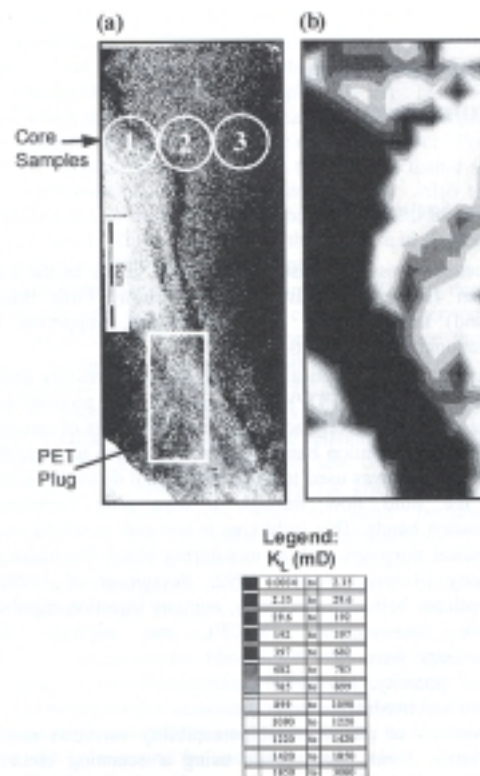


Figure 1. Heterogeneities across a deformation band in the Hopeman Sandstone. (a) Core photograph with sample and deformation band locations. The deformation band is shown as the light area running from top left to bottom right (b) Permeability profile of sandstone core in (a) using PDPK.

nitrogen permeabilities could be measured at each node of the grid using the method described in Jones [1992]. Slip-corrected (klinkenberg) permeabilities were obtained from the measured pressure decay data using a modified Darcy's equation [Jones, 1992] and plotted as a contour map (Fig. 1b). Figure 1a shows a photograph of an example of a slabbed rock showing the location of the deformation band and the position of the samples taken for other measurements reported in this work.

Two-dimensional porosities of thin-sections containing deformation bands were measured using Sigma Scan-Pro™ image analysis software. Samples of rock were taken from the slabbed rock and impregnated with an epoxy containing a blue dye. Thin-sections were made of these rock samples and imaged using a high quality digital colour camera. The image analysis software was used to separate the porous areas represented by blue dye from the matrix area using a colour/intensity cutoff. Two-dimensional porosity values were obtained in nine rectangular regions across each thin section, from which porosity profiles across the deformation bands were constructed (Fig. 2a).

Helium porosity and nitrogen permeability analyses were carried out on 3 (1 inch diameter) core plugs taken from the slabbed rock to characterize their mean porosity and permeability. These were taken from the host rock (sample 3),

deformation band zone (sample 1) and from the transitional area between them (sample 2), as shown in Fig. 1b. In addition, these three samples were subjected to the MICP technique, which provided the mean porosity of each sample together with their capillary pressure curves and their pore size distributions. Capillary pressures are a good measure of the sealing properties of a rock [Downey, 1984] and are significantly higher in the smaller pore radii of deformation bands compared to their host rock [Antonellini and Aydin, 1994]. Irreducible water saturation (S_{wi}) was calculated from this data, which was converted to oil or gas-brine data using appropriate contact angles and interfacial tensions. The conversion used was C_p (oil-brine) = 0.070 C_p (Air-Hg).

Positron emission scanning was used to analyze fluid flow through a cylindrical sandstone plug with a diameter of 3.5 cm and a length of 6.8 cm (13.4 cm³ pore volume) cut obliquely to the deformation band zone (Fig. 1a). This plug was completely sealed with Viton™ rubber and polycarbonate sleeves, and with Nylon™ 66 end caps equipped with fluid distribution grooves and pressure ports allowing a fluid to be passed axially through the plug without leakage around its sides.

Prior to PET scanning, the plug was saturated with distilled water to create a compatible medium for the isotopic solution. An aqueous solution with a 4×10^{-5} mCi/l concentration of

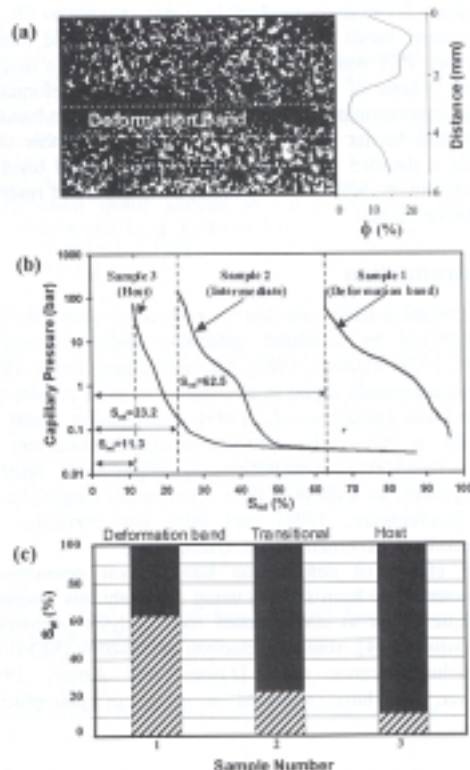


Figure 2. Conventional measurements on the three samples, locations shown in Fig. 1a. (a) Image analysis-derived porosity profile of a thin-section across a deformation band. (b) MICP-derived capillary pressure curves with S_{wi} variation in the samples. (c) Relationship between the storage capacity (black) and S_{wi} (hatched) in the samples.

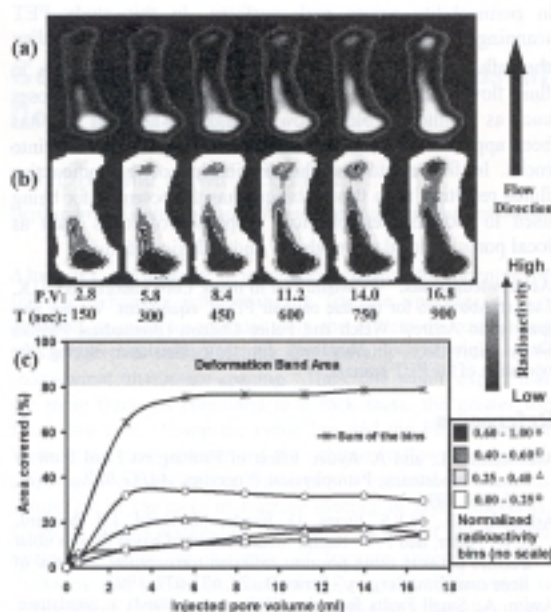


Figure 3. PET-scanning analysis of a radioactive fluid through a cross-section of a sandstone plug. (a) Frames showing the distribution of radioactive fluid as a function of injected pore volume (P.V) and time (T). (b) Distribution of different radioactive concentrations within normalized radioactivity bins. These bins are included in the legend (c) Percentage of the area covered by the radioactive fluid and by each of the four normalized radioactive concentration zones. The associated symbols are shown in the legend.

glucose containing very short half-life acting radioisotopes of fluorine-18 (^{18}F) was pumped at 15 ml/min into the sample. Atoms of this radioactive fluid occupying the pores emit positrons, which quickly interact with electrons to give two photons travelling in almost opposite directions. These photons are detected by a ring of sensors, taking account of the coincidence of their arrival. The detected photon data are then analyzed to produce a three-dimensional map of ^{18}F in the rock representing the pore space occupied by the injected radioactive fluid.

The radioactive fluid was flowed from the end of the core plug without the deformation band to the end which was

intersected by the oblique deformation band over 15 minutes, in which 30 PET scans were completed. Each frame contains enough information to reconstruct the 3D distribution of radioactive tracer at the time that each was taken.

4. Results

The methods of measuring permeability, PDPK and conventional core (nitrogen) permeametry are both 'klinkenberg-type', tests but they give different results. The high-resolution permeability image resulting from PDPK (Fig. 1b) shows a detailed permeability distribution across a deformation band zone. This is dominated by a swathe of permeabilities from 0.004 to 682 mD with a modal permeability of 3 mD, which coincides with the 2-3 cm thick zone of deformation bands as seen in the core image (Fig. 1a). Therefore the deformation band zone has low permeabilities, compared to the permeabilities of the transitional area and the host rock (682 to 3080 mD). This represents up to 6 orders of magnitude of permeability reduction (Table 1). However, conventional nitrogen permeabilities from three plugs, whose locations are shown in Fig. 1a, show a less dramatic permeability reduction of about 1 order of magnitude (Table 1). The main difference between these techniques is a result of the higher spatial resolution of the PDPK technique, resulting in measurements of much smaller volumes of rock. Hence, the PDPK technique observes significant permeability anisotropy at the mm-scale compared to core permeabilities measured at the cm-scale (e.g., nitrogen permeametry). Permeability heterogeneity using a much smaller grid in PDPK is expected to be even greater between the host rock and the deformation band.

Porosity heterogeneity at micro-scale (<1 mm) can be observed using SEM-BSEI in both the deformation band and host sandstone. In the former, this is a result of variations in mechanical deformation, which has reduced grain sizes and increased grain packing. Increased grain packing is aided by the reduction in sorting as observed in the experimental deformation bands of *Mair et al.* [2000]. However, in the host rock, mechanical deformation does not contribute to heterogeneity to the same extent.

Porosity measurements on core samples (at cm-scale) show a porosity reduction of up to 55% using helium porosimetry and mercury injection capillary pressure techniques (Table 1). The values measured by MICP are smaller than those derived using helium porosimetry, because mercury is not able to

Table 1. Porosity, Permeability and Irreducible Water Saturations for Samples containing Host Rock, Deformation Bands and a Transitional Zone between Host Rock and Deformation Bands.

Sample	Sample location	S_{wi} (%)		Porosity (%)		Klinkenberg Permeability (mD)	
		MICP	Helium	MICP	Image analysis	K_{R0}	PDPK
1	Deformation band	62.5	13.3	9.01	4 - 10	555	0.0034 - 397
2	Transitional	23.2	20.5	18.35	10 - 15	677	29.6 - 899
3	Host rock	11.3	25	19.95	15 - 21	1750	397 - 3080

reach the smallest pores in the sample. By comparison two-dimensional porosity mapping of a thin-section using image analysis shows a reduction up to 75% from the deformation band to the host rock (Table 1; Fig. 2a). With this type of measurement, a more detailed profile of the micro-scale (mm) porosity of the rock is obtained than with the use of 3D mean porosity, despite of the fact that the former depends on the thin-section orientation with respect to the orientation of the pores. Hence, differences in the porosity between the host rock and the deformation band are also dependent upon the scale of the measurement, but not as pronounced as in the case of permeability.

There is a considerable variation in capillary pressure and derived irreducible water saturation (S_{wi}) among the core plug samples (Fig. 2b; Table 1). The variation in S_{wi} among the three plug samples is the result of a decrease in the pore sizes or pore throat sizes in the deformation band compared to the host rock, which is reflected in an associated reduction of fluid storage capacity (Fig. 2c).

Positron emission tomography scanning was used to obtain the distribution of a doped radioactive aqueous fluid along an axial cross-section of a cylindrical core plug containing a deformation band zone as shown in Fig. 1a. Figure 3a shows the distribution of radioactive fluids in the core during the experiment as a function of injected pore volumes (PV) of doped fluid and time.

To monitor the movement of the radioactive fluid at different concentration levels with time, the area of the axial cross-section of the core plug was divided into four normalized radioactive bins representing different degrees of radioactivity (Fig. 3b). Variations in the extent of these bins depend on the local porosity of the rock, and the extent to which the local pore volume is saturated with radioisotope doped fluid. In general the radioactive fluid displaces the original fluid in the pores rapidly until 4 PV of radioactive fluid have been injected, invading approximately 72% of total area of an axial section of the plug (Fig. 3b). This proportion of the sample is the relatively highly porous and permeable host rock. After this stage, the rate of invasion reduced, which is reflected in smaller incremental increases in the area of the rock containing the injected fluid (Fig. 3c). The maximum area containing injected radioactive fluid is approximately 80% of the total area of the axial section through the sample. This is the result of the influence of the deformation band sealing off (compartmentalizing) the remaining 20% of the sample (Fig. 3c). Once the plug is predominantly saturated by radioactive fluid, there are internal displacements of different radioactive concentration bins within the plug, which may reflect the pores preferentially filled by the injected radioactive fluid. This can be seen in the variations of normalized radioactive bins with injected pore volume (Fig. 3b and 3c), which are much greater along the fluid direction than normal to this.

5. Conclusions

The results of the PDPK and PET scanning techniques demonstrate the influence of deformation bands as a significant barrier to fluid flow. This is the result of considerable reduction in porosity and permeability into the deformation band zone, which is related to a reduction in the sandstone storage capacity. These differences in the porosity and permeability between the host rock and the deformation band are dependent at different levels upon the scale of the measurement of the technique used.

High resolution PDPK mapping of deformation bands has significant application in determining micro-scale variations in permeability across rock surfaces. In this study PET scanning has proven to be a successful technique to visualize the influence of deformation bands as potential barriers to fluid flow, although it is normally used for medical purposes such as monitoring blood flow through the heart. It also has been applied in tracing the migration of radioactive fluids into rocks. In further studies, the distribution of the radioactive fluids resulting from this technique has the potential for being used to monitor petrophysical properties of rocks such as local porosity, local permeability and diffusion of fluids.

Acknowledgments. We would like to thank Core Laboratories U.K. Ltd. at Aberdeen for the use of their PDPK equipment. We are also grateful to Andrew Welch and Felice Chilcott (Biomedical Physics Dept., University of Aberdeen) for their assistance during the operation of the PET scanner.

References

- Antonellini, M., and A. Aydin, Effect of Faulting on Fluid Flow in Porous Sandstones; Petrophysical Properties. *AAPG Bull.*, 78 (3), 355-377, 1994.
- Ashcroft, G.P., N.T.S. Evans, D. Roeda, M. Dodd, J.R. Mallard, R.W. Porter, and F.W. Smith, Measurement of blood flow in tibial fracture patients using positron emission tomography. *Journal of Bone and Joint Surgery - Series B*, 74, 673-677, 1992.
- Aydin, A., Small Faults formed as Deformation Bands in Sandstone. *Pure Appl. Geophys.*, 116, 913-930, 1978.
- Beach, A., A.I. Welton, P.J. Brockbank, and J.E. McCullum, Reservoir damage around faults: outcrop examples from the Suez rift. *Petroleum Geoscience*, 5, 109-116, 1999.
- Besson, J.A.O., J.R. Crawford, N.T.S. Evans, H.G. Gemmill, and D. Roeda, PET imaging in Alzheimer's disease. *Journal of the Royal Society of Medicine*, 85 (4), 231-234, 1992.
- Downey, M.W., Evaluating seals for hydrocarbon accumulations. *AAPG Bull.*, 68, 1752-1763, 1984.
- Edwards, H.E., A.D. Becker, and J.A. Howell, Compartmentalization of an aeolian sandstone by structural heterogeneities: Permian-Triassic Hopeman Sandstone, Moray Firth, Scotland. *From North, C.P. & Prasser, D.J. (eds), 1993. Characterisation of Fluvial and Aeolian Reservoirs, Geol. Soc. Lond. Spec. Publ.*, 73, 339-365, 1993.
- Fisher, Q.J., and R.J. Knipe, Fault sealing processes in siliclastic sediments. *From Jones, G., Fisher, Q.J. and Knipe, R.J. (eds), 1998. Faulting, Fault Sealing and Fluid Flow in Hydrocarbon Reservoirs. Geol. Soc. Lond. Spec. Publ.*, 147, 117-135, 1998.
- Fossen, H., and J. Hesthammer, Deformation bands and their significance in porous sandstone reservoirs. *Research article, First break*, 16, 21-25, 1998.
- Frostick, L., I. Reid, J. Jarvis, and H. Eardley, Triassic Sediments of the Inner Moray Firth, Scotland: early rift deposits. *J. Geol. Soc. Lond.*, 145, 235-248, 1988.
- Jones, S.C., The Profile Permeameter; A new fast accurate Minipermeameter, Paper SPE 24757 presented at the 1992 SPE Technical Conference and Exhibition, Washington, Oct 4-7, 1992.
- Mair, K., I. Main and S. Elphick, Sequential growth of deformation bands in the laboratory. *J. Struct. Geol.*, 22, 25-42, 2000.
- Pitman, E.D., Effect of Fault-Related Granulation on porosity and permeability of Quartz Sandstones, Simpson Group (Ordovician), Oklahoma. *AAPG Bull.*, 65 (11), 2381-2387, 1981.

S. Ogilvie, Department of Geology and Petroleum Geology, University of Aberdeen, King's College, Aberdeen AB24 3UE, Scotland (e-mail: s.ogilvie@abdn.ac.uk).

J. Orriso, Department of Geology and Petroleum Geology, University of Aberdeen, King's College, Aberdeen AB24 3UE, Scotland (e-mail: j.orriso@abdn.ac.uk).

P. Glover, Department of Geology and Petroleum Geology, University of Aberdeen, King's College, Aberdeen AB24 3UE, Scotland (e-mail: p.glover@abdn.ac.uk).

(Received Feb 11, 2000; revised September 14, 2000; accepted October 17, 2000)